Supplement of Biogeosciences, 23, 2451–2476, 2026
https://doi.org/10.5194/bg-23-2451-2026-supplement

Biogeosciences Open Access EGU

Supplement of

Forest diversity and environmental factors shape contrasting soil-litter fluxes of biogenic volatile organic compounds and methane in three central Amazonian ecosystems

Débora Pinheiro-Oliveira et al.

Correspondence to: Débora Pinheiro-Oliveira (dpinheiro@bgc-jena.mpg.de) and Eliane Gomes Alves (egomes@bgc-jena.mpg.de)

Supplementary Material

S1. Soil Texture

Table S1. Soil particle size distribution in three forest types in central Amazonia. The data represents the percentage composition of total sand, silt, and clay. Each sample is a composite sample from two nearby points in the field. AR = Ancient River Terrace Forest, WS = White Sand Forest, Up = Upland Forest.

Soil Texture				
Forest type	samples	Sand (%)	Silt (%)	Clay (%)
AR	TR1.1	45.449	37.801	16.75
AR	TR1.2	45.449	37.801	16.75
AR	TR1.3	47.639	30.061	22.30
AR	TR1.4	47.639	30.061	22.30
AR	TR1.5	12.38	56.22	31.40
AR	TR1.6	12.38	56.22	31.40
AR	TR2.1	41.543	34.457	24.00
AR	TR2.2	41.543	34.457	24.00
AR	TR2.3	42.078	35.422	22.50
AR	TR2.4	42.078	35.422	22.50
AR	TR2.5	47.17	28.68	24.15
AR	TR2.6	47.17	28.68	24.15
WS	CP1.1	46.15	52.35	1.50
WS	CP1.2	46.15	52.35	1.50
WS	CP1.3	50.07	47.68	2.25
WS	CP1.4	50.07	47.68	2.25
WS	CP1.5	74.398	24.252	1.35
WS	CP1.6	74.398	24.252	1.35
WS	CP2.1	76.599	22.301	1.10
WS	CP2.2	76.599	22.301	1.10
WS	CP2.3	24.134	74.616	1.25
WS	CP2.4	24.134	74.616	1.25
WS	CP2.5	73.883	24.517	1.60
WS	CP2.6	73.883	24.517	1.60
Up	TF1.1	23.011	26.139	50.85
Up	TF1.2	23.011	26.139	50.85
Up	TF1.3	12.595	30.255	57.15
Up	TF1.4	12.595	30.255	57.15
Up	TF1.5	12.698	38.602	48.70
Up	TF1.6	12.698	38.602	48.70
Up	TF2.1	11.892	40.858	47.25

Up	TF2.2	11.892	40.858	47.25
Up	TF2.3	10.194	32.506	57.30
Up	TF2.4	10.194	32.506	57.30
Up	TF2.5	9.587	35.413	55.00
Up	TF2.6	9.587	35.413	55.00

S2. Calibration gas composition

Table S2. Multi-component calibration mixture in synthetic air, as used for the calibration of the PTR-QMS. Uncertainty is a conservative estimate of the combination of gravimetric preparation and analysis uncertainties.

Compound	CAS#	Concentration (ppb)	Uncertainty
Formaldehyde	50-0-0	992	5%
Acetaldehyde	75-07-0	426	5%
Methanol	67-56-1	521	5%
Ethanol	64-17-5	528	5%
Acetonitrile	75-05-8	523	5%
Acetone	67-64-1	497	5%
Isoprene	78-79-5	468	5%
DMS	75-18-3	487	5%
a-Pinene	80-56-8	488	5%
Camphene	79-92-5	504	5%
B-Pinene	18172-67-3	512	5%
a-Phellandrene	4221-98-1	432	5%
3-Carene	13466-78-9	458	5%
Limonene	5889-54-8	489	5%
o-Cymene	527-84-4	481	5%
y-Terpinene	99-85-4	476	5%
B-Caryophyllene	87-44-5	98.3	5%
a-Humulene	6753-98-6	95.2	5%

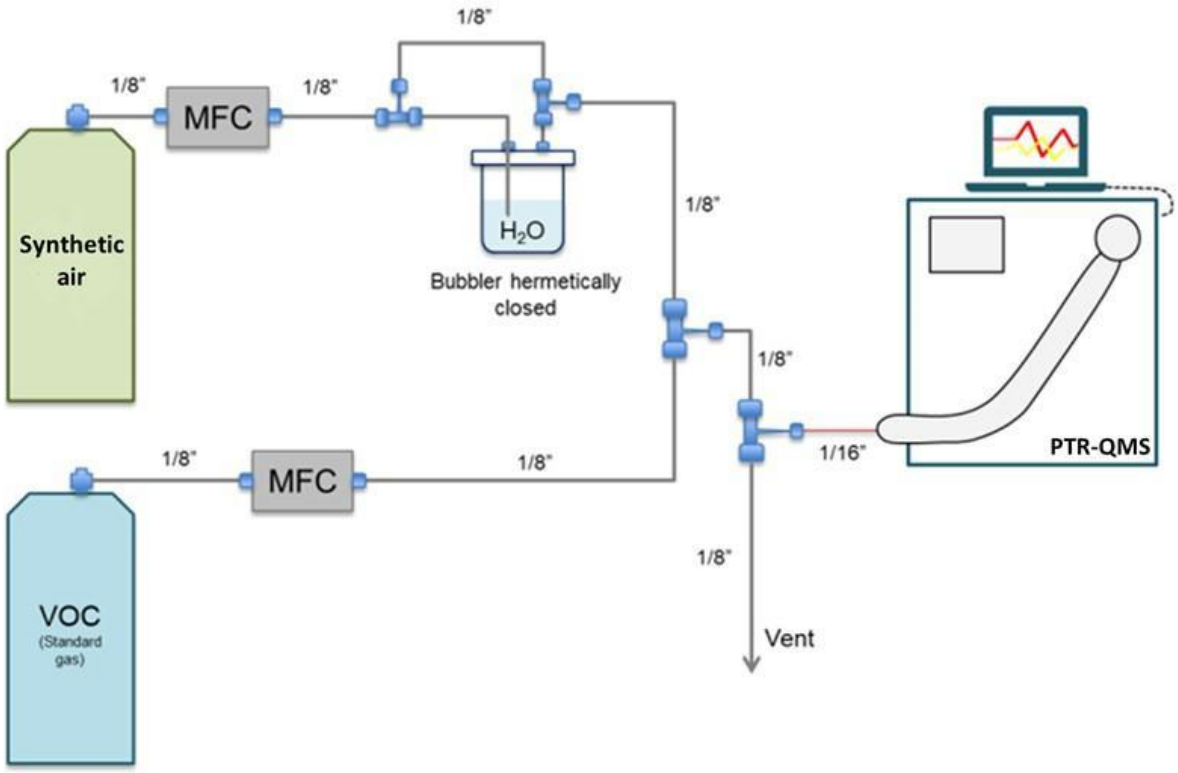

Figure S1. PTR-QMS calibration setup scheme, the VOC standard gas is as described in Table S2, figure adapted from Caetano (2022).

S3. BVOC & GHG flux calculation

Fluxes were calculated using the closed chamber formulation, as given in equation 1 (manuscript, Section 2.5). It should be considered that the chamber was operated under a continuous flow (0.5 L min^{-1}), which introduces a constant small dilution of the accumulating BVOCs and GHG. Therefore, the system is formally a non-steady-state flow-through chamber rather than a strictly static chamber. Using the closed chamber formula instead of the non-steady-state flow-through chamber formula leads to an underestimation of 25%, as shown below.

For a flow-through chamber with volume V, surface area A, flow rate Q, and enclosure time t, the transient mass balance gives:

$$C(t) - Cin = \frac{FA}{Q}\,(1 - e^{-Qt/V}) \qquad \text{(S1)}$$

Solving for flux yields the non-steady-state formulation:

$$Fopen = \frac{Q}{A}\frac{\Delta C\,(t)}{1-e^{-Qt/V}}\frac{P}{RT} \quad \text{(S2)}$$

where $\Delta C(t)=C(t)-Cin$, P is pressure, T is temperature, and R is the gas constant.

In contrast, the closed chamber formulation assumes linear accumulation:

$$Fclosed = \frac{V}{A}\frac{\Delta C(t)}{t}\frac{P}{RT} \quad \text{(S3)}$$

The relative bias introduced by applying the closed formulation to a flow-through system depends only on the dimensionless term Qt/V:

$$\frac{Fclosed}{Fopen} = \frac{1-e^{-Qt/V}}{Qt/V} \quad \text{(S4)}$$

For the present study:

$t = 25$ min

$Q = 0.5$ L min^{-1}

$V = 21$ L

This gives:

$$\frac{Qt}{V} = 0.595$$

and therefore:

$$\frac{Fclosed}{Fopen} = 0.754$$

indicating that the closed chamber approach underestimates the flux by approximately:

$$1 - 0.754 = 0.246 \approx 25\%$$

Thus, for the chamber configuration used here (A = 0.0855 m^2, V = 21L, Q = 0.5 L min^{-1}, enclosure time 25 min), the expected underestimation due to assuming closed chamber conditions is on the order of 25%. Importantly, this correction depends only on the Qt/V ratio and is independent of the absolute magnitude of the flux. The reported fluxes should therefore be considered conservative estimates, and this potential bias does not affect the main conclusions of the study.

S4. Gas Chromatography - Time of Flight Mass Spectrometer (GC-TOF-MS) analysis

S4.1 GC-TOF-MS: Material & Methods

After determining gas mixing ratios on the PTR-QMS and the Los Gatos analyzer, samples were collected onto cartridges (stainless steel tubes filled with Tenax TA and Carbograph 5 TD adsorbents, Markes International, UK) at a rate of 200 sccm for 10 min, which resulted in 2L air samples for compound identification and quantification analyses with the GC-TOFMS. The cartridges were stored in an air-conditioned room for up to six months until they were analyzed.

Samples were examined with a thermal-desorption gas chromatograph coupled to a time-of-flight mass spectrometer (TD-GC-TOF-MS; Bench TOF Tandem Ionisation, Markes International, UK). A complete description of the instrument, analytical procedure, and performance is available in Zannoni et al. (2020a, 2020b). In the TD-GC-TOF-MS, the analytes are desorbed from the sampling tubes using two sequential stages, performed at 250°C for 10 minutes, then carried by a flow of He into the separating column in the gas chromatograph. The column is a dimethyl TBS β-cyclodextrin column (0.25µm, 0.25mm ID, 30 mL, from MEGA, Italy), which separates the analytes according to volatility and enantiomeric configuration. The separation method was specifically designed for the separation of chiral monoterpenes ($C_{10}H_{16}$) and sesquiterpenes ($C_{15}H_{24}$) and consisted of an initial 5 min when the oven temperature was held at 40°C, after which it was increased at a rate of 1.5 °C/min from 40°C to 150°C. Finally, the temperature increased further at a rate of 30°C/min from 150°C to 200°C. Detection was performed by a Time-of-Flight Mass Spectrometer, which fragments the analytes through electron impact ionization at -70 eV for quantification and identification of the chemical species. Identification of the main chemical

compounds was obtained by comparing the MS spectra with the MS library for the same ionization energy (NIST library), by injection of a calibration gas standard mixture (19 biogenic volatile organic compounds provided by Apel Riemer, USA), and by use of liquid standards. Chromatogram peak areas were integrated through TOF-DS software provided with the instrument (Markes International, UK). The standard gas used is a certified concentrated mixture (~100 ppbv) of 19 BVOCs, including, among the other species, four pairs of chiral terpenoids (α-pinene, β-pinene, limonene, linalool), isoprene, and one sesquiterpene (β-caryophyllene). The GC-TOF sensitivity was quantified by measuring the concentration of BVOCs in standard sorbent tubes filled with 2 L of gas standard diluted in a pure synthetic air flow with four dilution steps to achieve concentrations in the range of 0.05-1 ppb. Such calibrations were performed before or at the end of each sample batch. The obtained calibration factors were confirmed using standard cartridges containing a known BVOC concentration (~0.150 ppb) in a workflow, with a standard cartridge measured for every 10 samples analyzed. The standard cartridges were analyzed in this way to determine the analysis precision (including any mass spectrometer drift), which was quantified at 22% (Zannoni *et al*. 2020a and Zannoni *et al.* 2020b).

S4.2 GC-TOF-MS: Results

For all BVOC fluxes studied, emissions were highest in the White Sand Forest. Notably, some BVOCs were detected exclusively in the White Sand Forest and were completely absent from the other forest types (Figure S2).

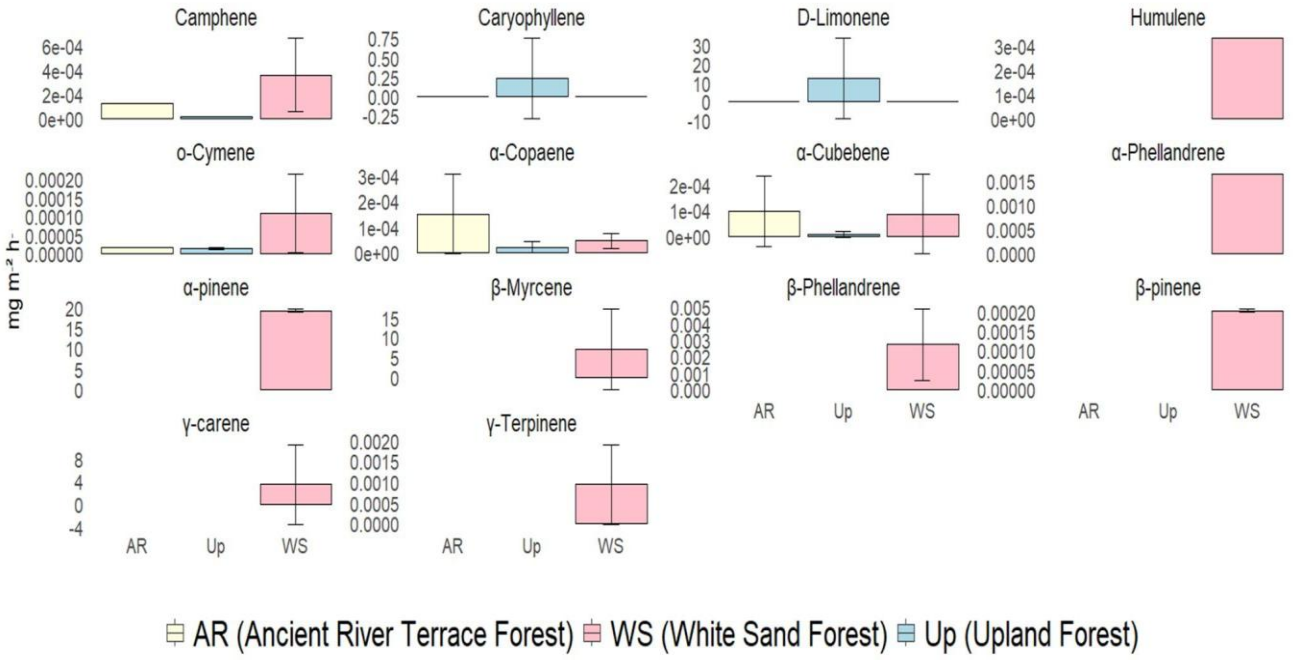

104

105 **Figure S2.** BVOC Fluxes from the soil and litter across the three forest types. Bar plot of the 12 samples
106 from each environment.

107

108 **S5. Linear Models (LM)**

109 **S5.1 White sand forest fluxes and their potential predictors**

110 Firstly, we investigated the relationships among the potential predictor variables in the white sand
111 forest ecosystem, independent of their relation to gas fluxes. These predictor variables include soil
112 and litter characteristics, microbial biomass, soil moisture, and temperature. The Pearson
113 correlations for these variables are presented in Figure S3a, which highlights the interactions and
114 dependencies between environmental drivers only.

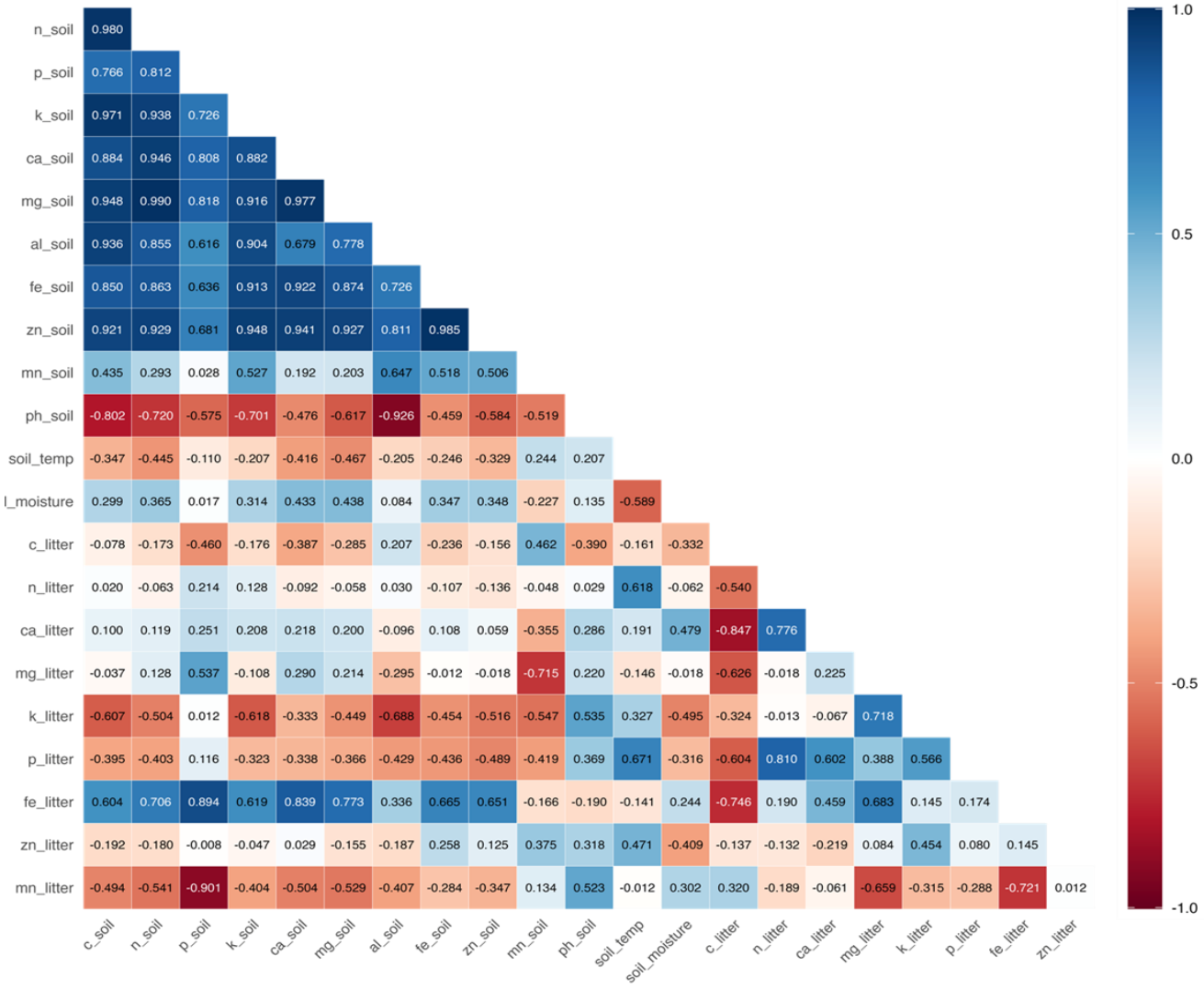

Figure S3a. Heatmap for the Pearson correlation coefficients for the potential predictors of fluxes in the white sand forest. N = 12.

Secondly, we analyzed the correlations between the potential predictor variables and the response variables, which are the BVOC and GHG fluxes measured in this study. The Pearson correlations for these relationships are shown in Figure S3b, which specifically highlights how the fluxes of BVOCs and GHGs are associated with environmental drivers. This distinction between Figure S3a (predictor-predictor correlations) and Figure S3b (predictor-response correlations) underscores the separate analyses of interactions among environmental variables and their direct associations with gas fluxes.

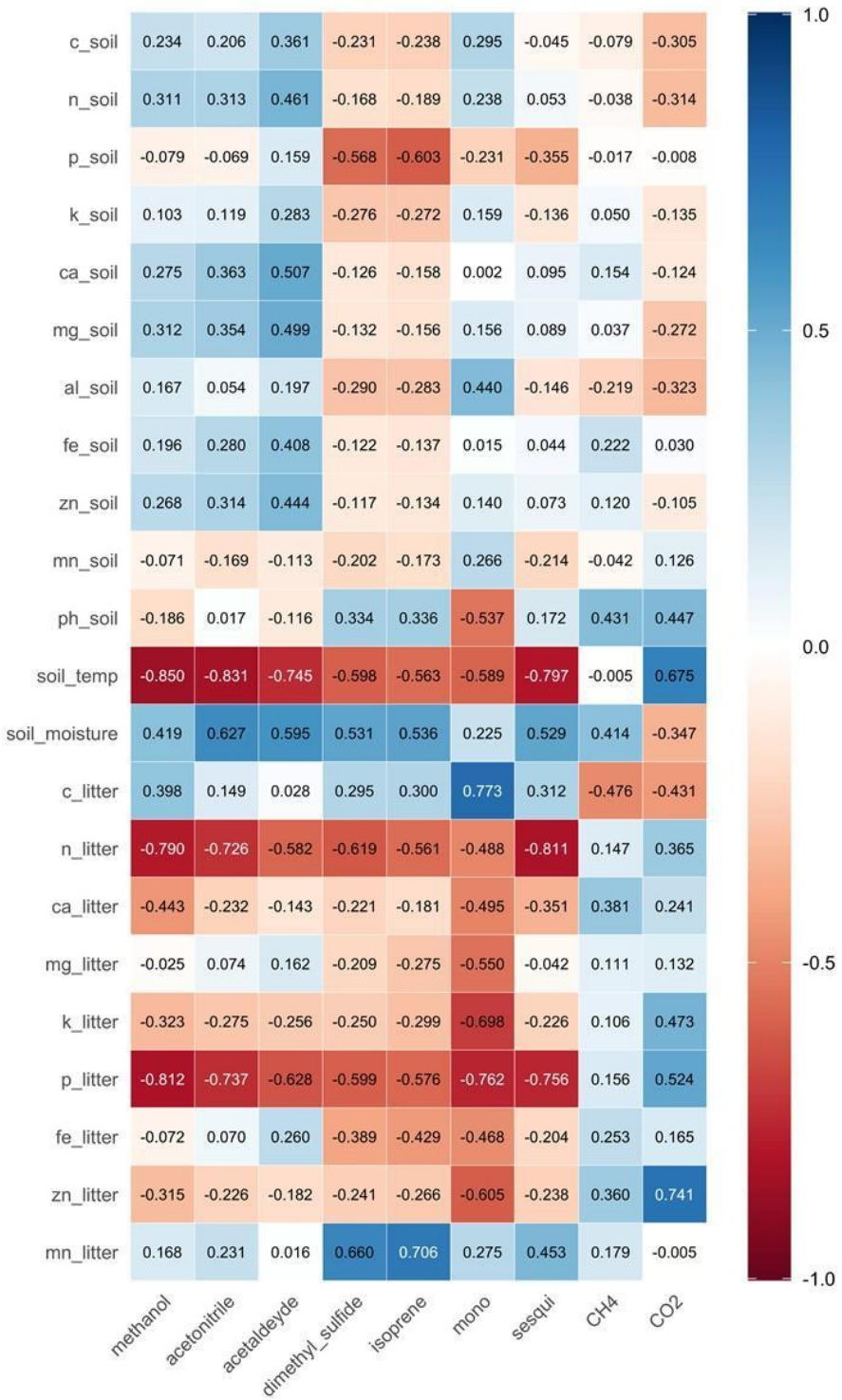

125

126 **Figure S3b.** Heatmap for the Pearson correlation coefficients for the correlation between gas
127 fluxes and their potential predictors in the white sand forest. N = 12.

S5.2 Ancient River Terrace Forest fluxes and their potential predictors

Initially, our investigation into the ancient river terrace forest ecosystem centered on delineating the intricate relationships among its key predictor variables. These variables encompass a range of soil and litter characteristics, microbial biomass metrics, and essential environmental parameters such as soil moisture and temperature. The outcomes of these Pearson correlation analyses are visually encapsulated in Figure S4a, which specifically illuminates the interdependence and patterns observed exclusively among these potential environmental drivers.

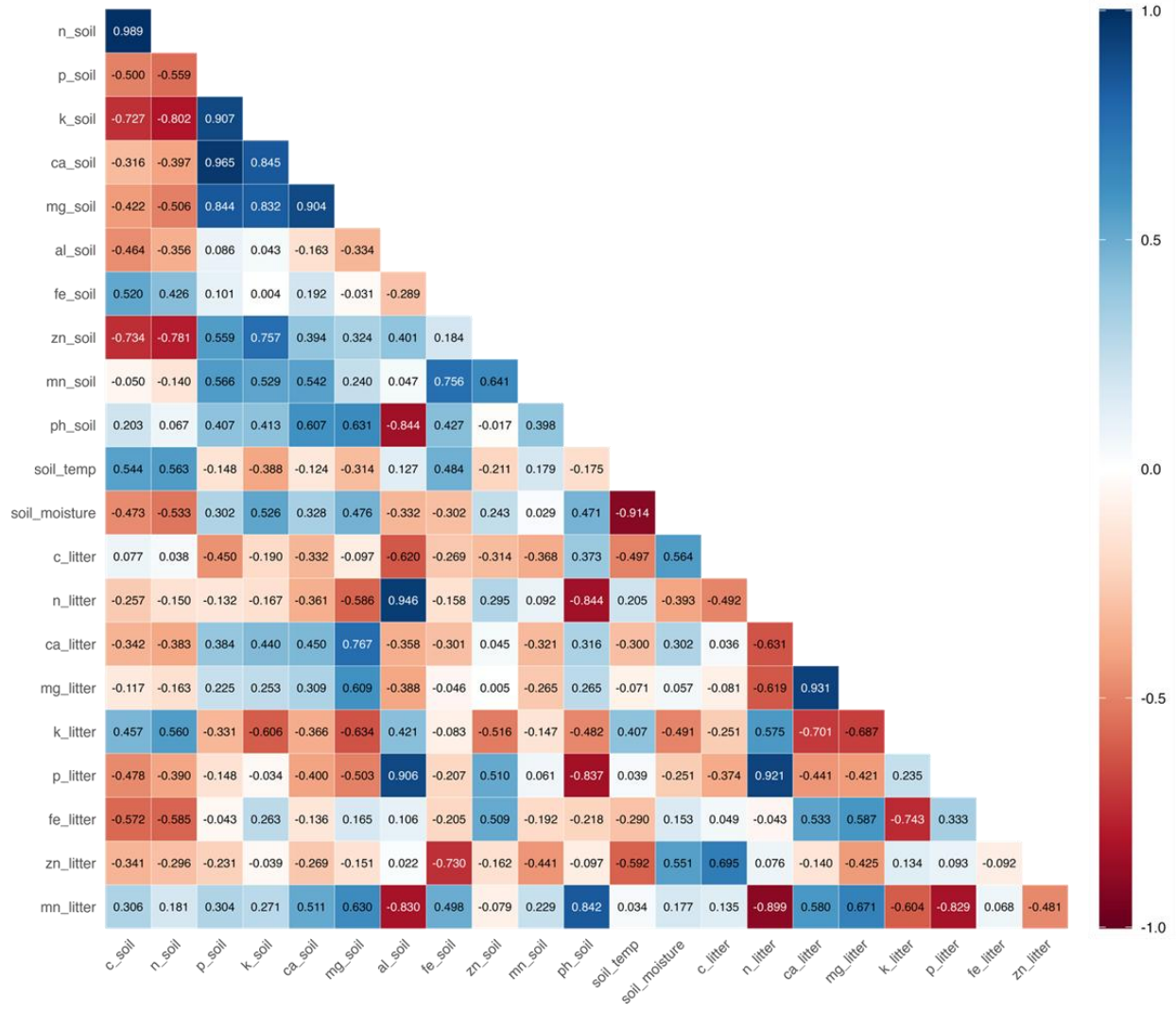

Figure S4a. Heatmap for the Pearson correlation coefficients for the potential predictors of gas fluxes in the ancient river terrace forest. N = 12.

Following this, direct correlations were examined between these same predictor variables and the measured response variables: BVOC and GHG fluxes. Figure S4b illustrates these Pearson correlations, highlighting specific associations between environmental factors and observed magnitudes of BVOC and GHG exchange. By presenting Figure S4a for predictor-predictor correlations and Figure S4b for predictor-response correlations, the goal was to provide a clear, two-level understanding of the underlying factors influencing gas fluxes in this type of forest.

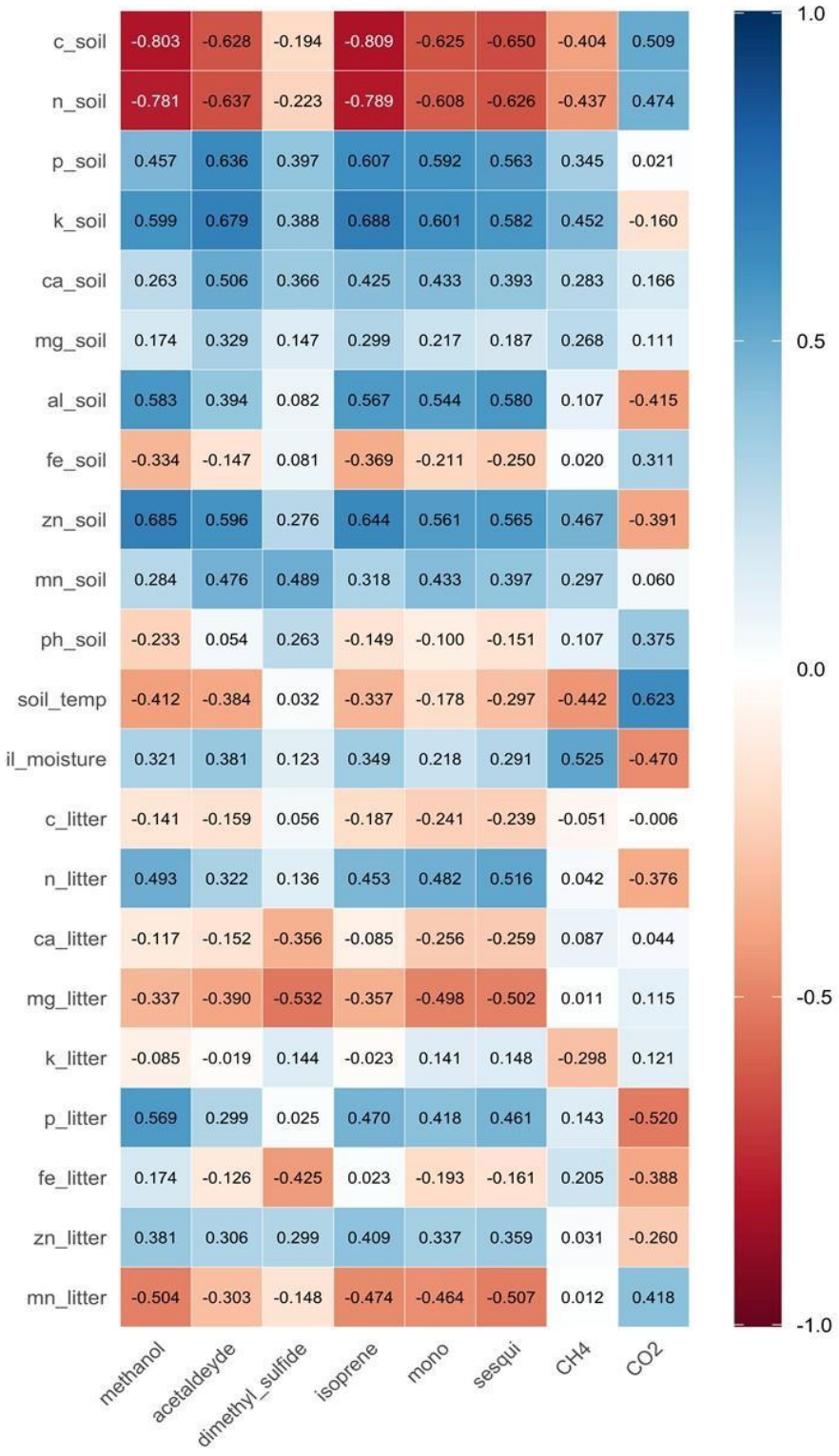

145

146 **Figure S4b**. Heatmap for the Pearson correlation coefficients for the correlation between gas
147 fluxes and their potential predictors in the ancient river terrace forest. N = 12.

S5.3 Upland forest fluxes and their potential predictors

For the upland forest, we started by exploring the interrelationships existing between its various potential predictor variables. These predictors comprise elements such as soil and litter properties, indicators of microbial activity, and critical environmental conditions like soil moisture and temperature. The Pearson correlation coefficients that define these connections are systematically displayed in Figure S5a, providing a comprehensive overview of the intrinsic linkages among these environmental factors.

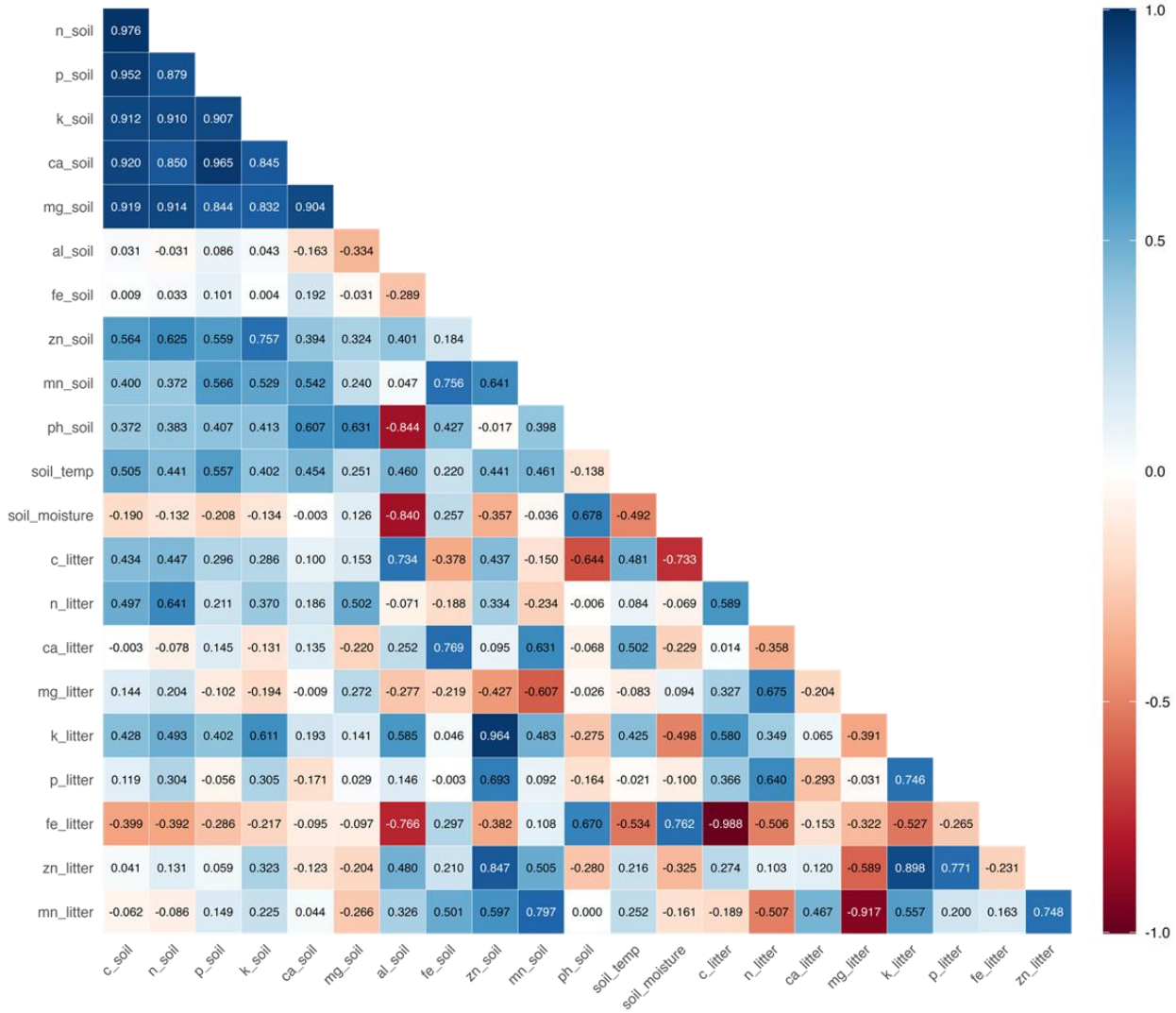

Figure S5a. Heatmap for the Pearson correlation coefficients for the potential predictors of gas fluxes and their potential predictors in the upland forest. N = 12.

Subsequently, the focus shifted to quantifying the correlations between these identified predictor variables and the study's response variables, which are BVOC and GHG fluxes. Figure S5b graphically represents these Pearson correlations, offering specific insights into how variations in environmental factors are associated with patterns of BVOC and GHG fluxes in the upland forest. This dual visualization, with Figure S5a detailing the links between predictors and Figure S5b focusing on the interactions between predictors and responses, allows for a nuanced interpretation of the factors driving gas fluxes.

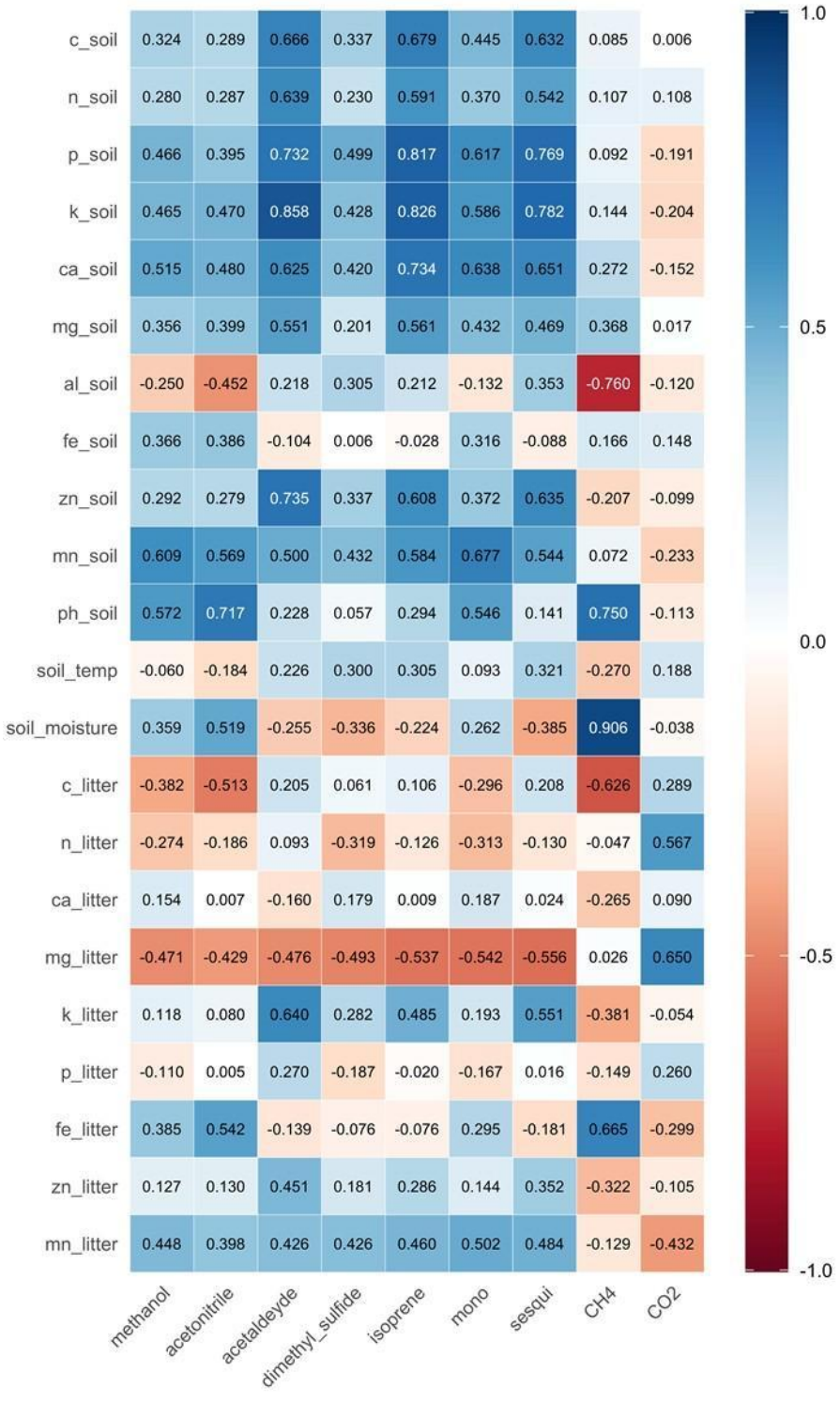

Figure S5b. Heatmap for the Pearson correlation coefficients for the correlation between gas fluxes and their potential predictors in the upland forest. N = 12.

S6. Tangled Influences of Soil Moisture and Temperature on BVOC and CH_4 Fluxes

S6.1 Relation between soil moisture and soil temperature (all forest types)

Generally, drier soil conditions were associated with warmer soil temperatures (Figure S6), with coefficients of determination (R^2) of 0.82 (AR), 0.28 (WS), and 0.17 (UP). This interdependent behavior complicates the interpretation of direct relationships between soil moisture, soil temperature, and soil fluxes (Figure S7).

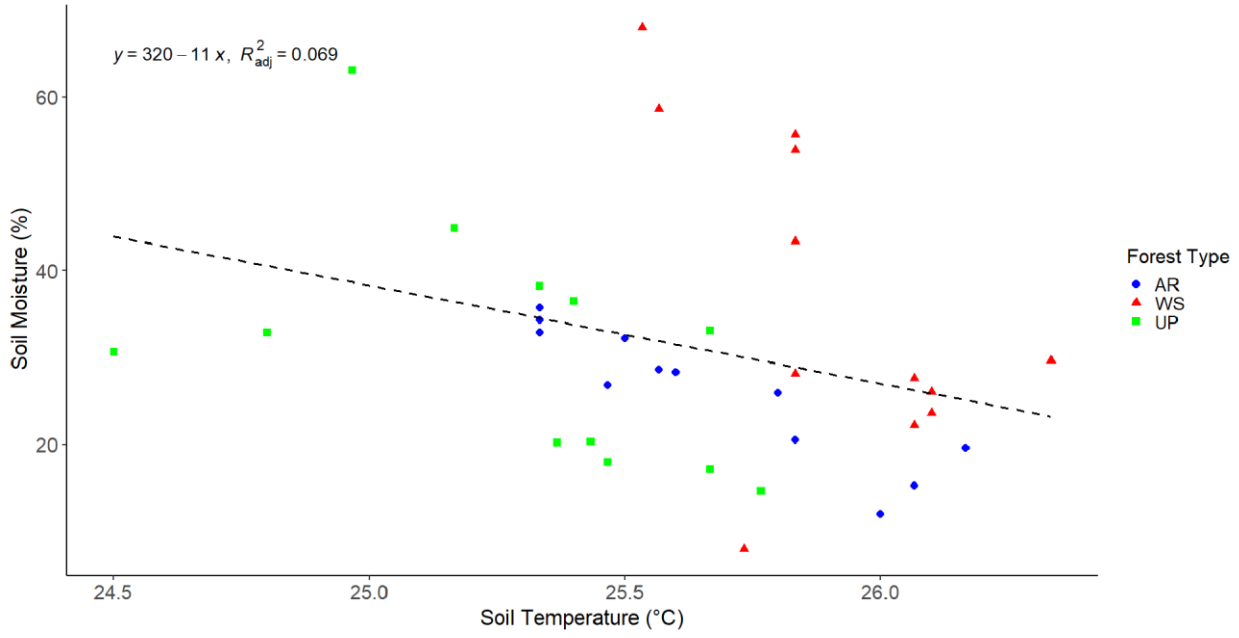

Figure S6. Relation between soil moisture and soil temperature in all forest types (AR, WS and UP), average of five measurements taken in the topsoil. The dashed line represents the linear regression fitted to the data, indicating the general trend of the relationship between soil moisture and soil temperature. This regression model was built based on 36 observations.

S6.2 Relation between soil temperature, soil moisture, and CH_4 fluxes (all forest types)

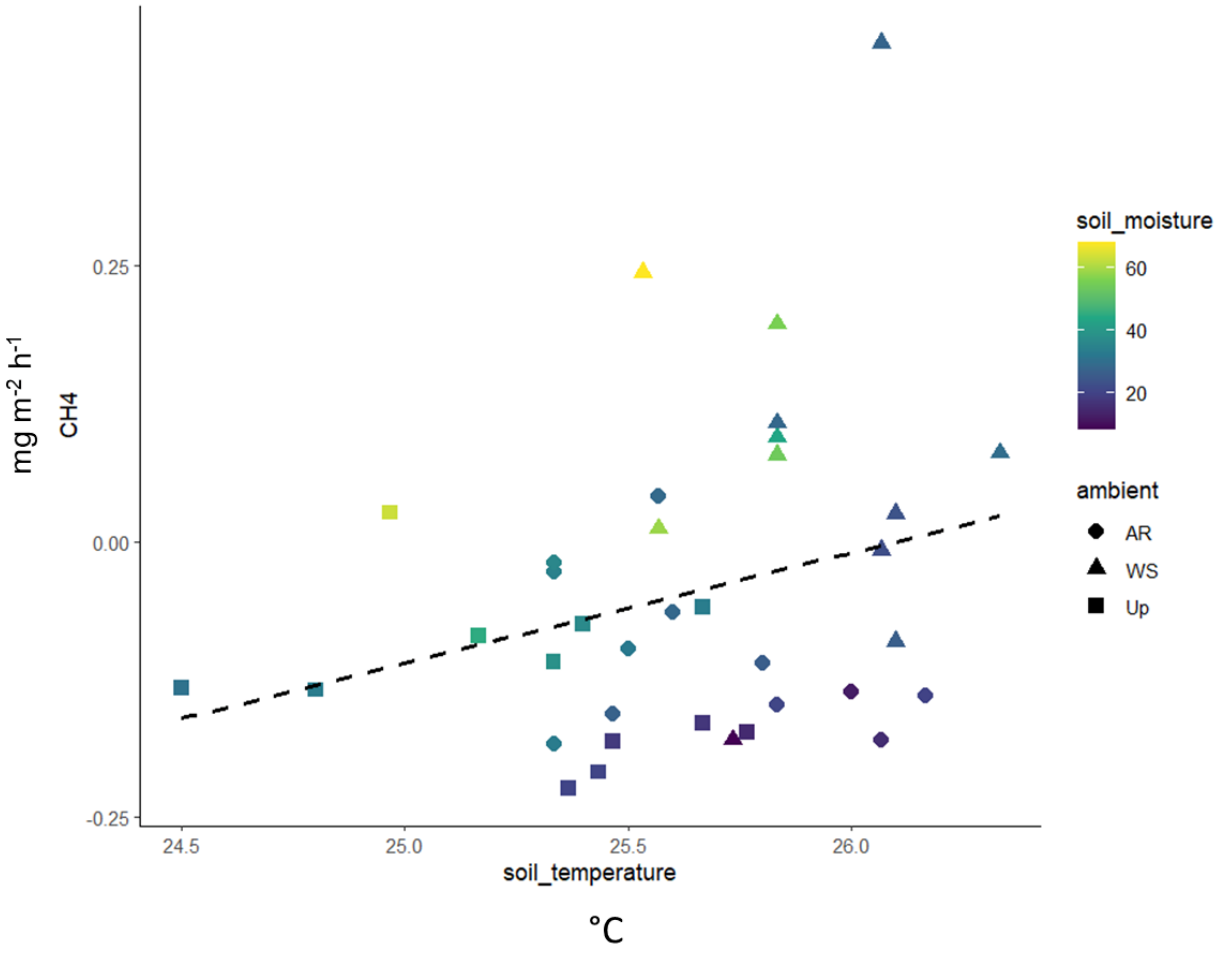

Figure S7. CH_4 flux from the soil and litter in the different forest types. The figure shows the relationship between soil-litter CH_4 flux (mg m^{-2} h^{-1}, y-axis), soil temperature (x-axis), and soil moisture (color bar), where soil moisture and soil temperature values are an average of five measurements taken in the topsoil. The dashed line represents the linear regression fitted to the data, indicating the general trend of the relationship between soil temperature, moisture, and CH_4 fluxes. This regression model was built based on 36 observations.

S7. Spatial variability

Although we attempted to select homogeneous and representative transects within each forest type, we still observed differences in soil temperature and soil moisture between transects of the same forest type, even when measurements were taken at the same time of day and only one day apart

(Figure S8). For instance, in the upland forest, transect 1 was drier and warmer than transect 2. In the white sand forest, transect 2 was colder and wetter than transect 1, likely partly due to a rain event shortly before the measurements. CO_2 and CH_4 fluxes also exhibited considerable spatial variability between and within transects (Figure S9). For BVOC fluxes, transects within the same forest type even showed opposite flux directions, for example, with mostly uptake and mostly emission in respectively transect 2 and transect 1 of the ancient river terrace forest (Figure S10).

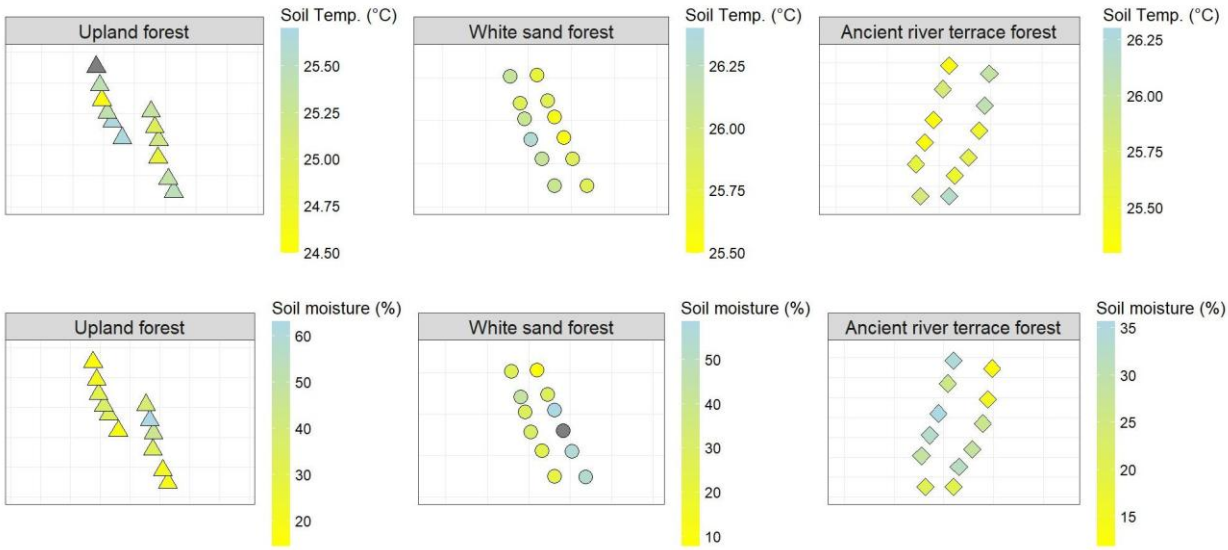

Figure S8. Map showing the soil temperature (°C) (upper row) and soil moisture (%) (lower row) for the two transects in each of the three forest types: Up, WS, and AR. Each transect contained six sampling points, totaling 12 measurement points per forest type. Left - Transect 1; Right – Transect 2.

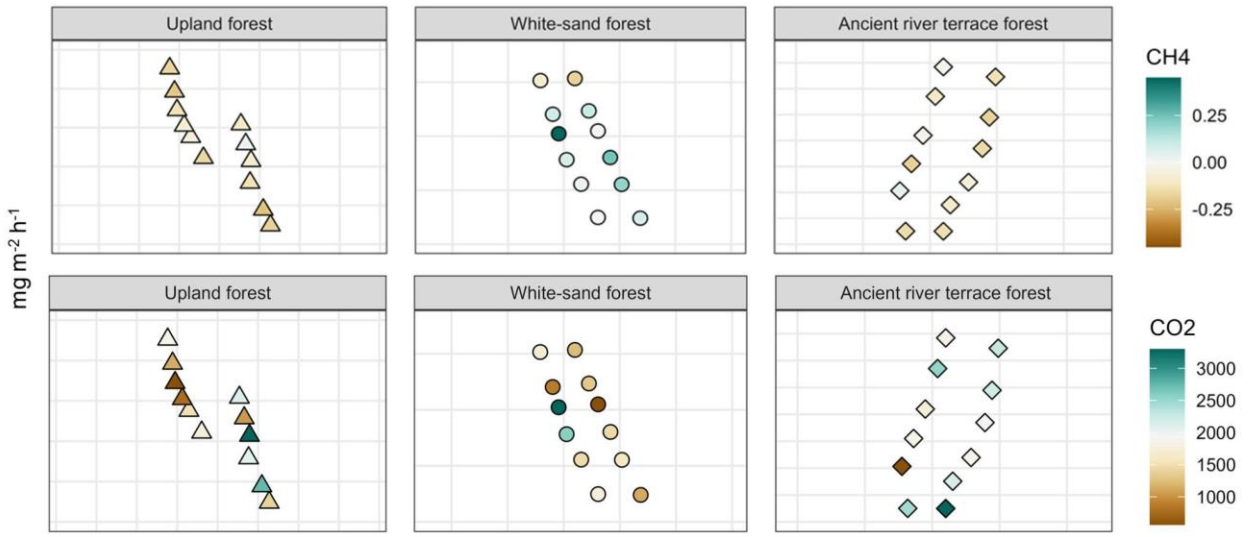

Figure S9. Map of the points collected showing the flux of GHG - methane (CH_4) (upper row) and CO_2 (lower row) in each of the three forest types: Up, WS, and AR. Each transect contained six sampling points, totaling 12 measurement points per forest type. Left - Transect 1; Right - Transect 2. The gas flux data are expressed in mg m^{-2} h^{-1}.

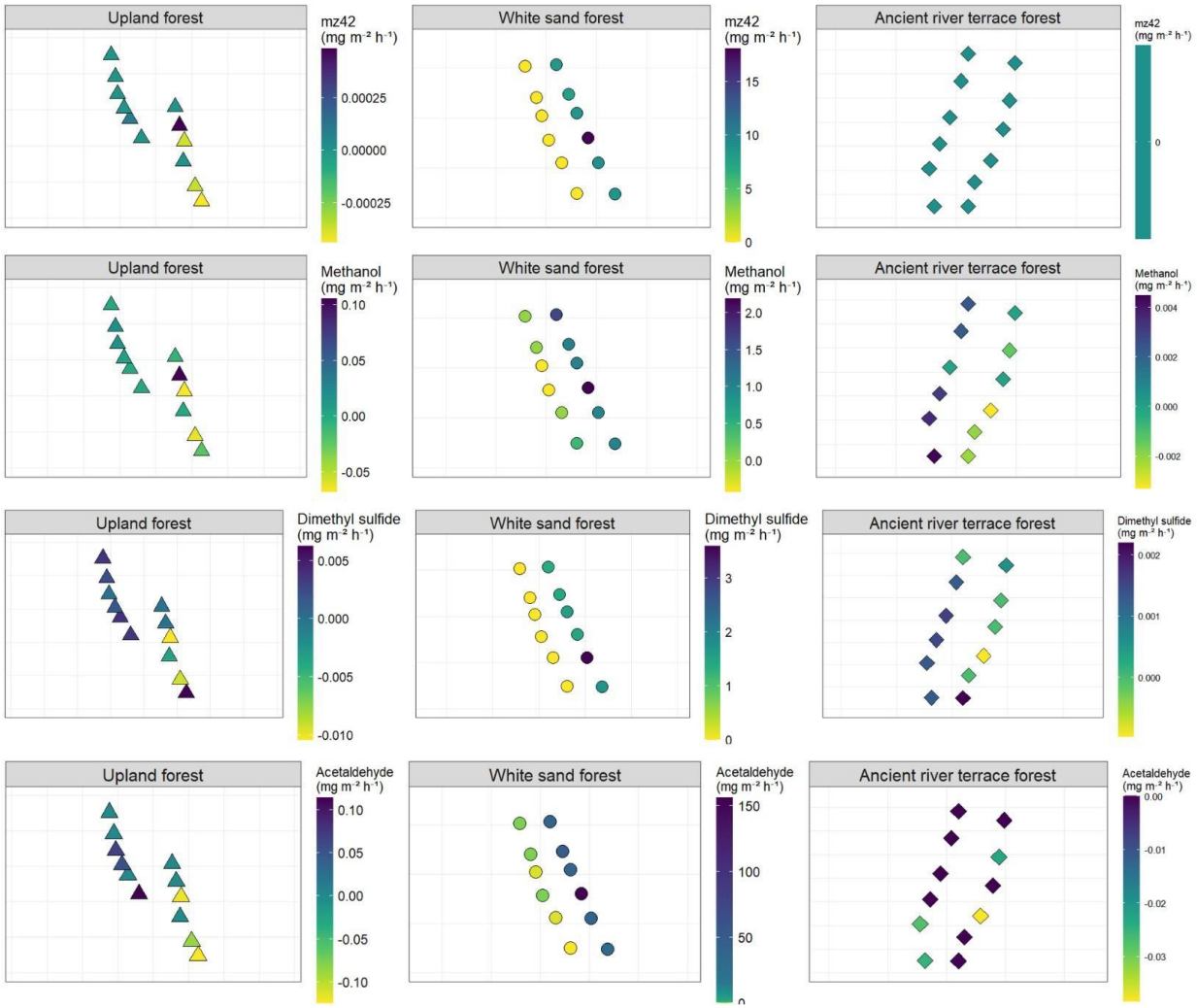

Figure S10. Map of the points collected showing the BVOC fluxes (mg m^{-2} h^{-1}) in each of the three forest types: Up, WS, and AR. Each transect contained six sampling points, totaling 12 measurement points per forest type. Left - Transect 1; Right - Transect 2.